

Manganese-induced long-range lattice disorder and vacancy formation in metal-organic chemical vapor deposition grown and ion-implanted $\text{Ga}_{1-x}\text{Mn}_x\text{N}$

William E. Fenwick, Ali Asghar, Shalini Gupta, and Hun Kang
School of Electrical and Computer Engineering, Georgia Institute of Technology, Atlanta, Georgia 30332-0250

Martin Strassburg and Nikolaus Dietz
Department of Physics and Astronomy, Georgia State University, Atlanta, Georgia 30302-4106

Samuel Graham
School of Mechanical Engineering, Georgia Institute of Technology, Atlanta, Georgia 30332-0405

Matthew H. Kane and Ian T. Ferguson^{a)}
School of Electrical and Computer Engineering, Georgia Institute of Technology, Atlanta, Georgia 30332-0250 and School of Materials Science and Engineering, Georgia Institute of Technology, Atlanta, Georgia 30332-0245

(Received 5 December 2005; accepted 3 April 2006; published 23 June 2006)

The structural properties and lattice dynamics of $\text{Ga}_{1-x}\text{Mn}_x\text{N}$ were studied for Mn concentrations from 0.0% to 1.5%. $\text{Ga}_{1-x}\text{Mn}_x\text{N}$ layers were fabricated by either Mn incorporation during the metal-organic chemical vapor deposition (MOCVD) growth process or by postgrowth ion implantation into MOCVD-grown GaN epilayers. The crystalline integrity and the absence of major second phase contributions were confirmed by high-resolution x-ray diffraction analysis. Raman spectroscopy showed that increased Mn incorporation in the epilayers significantly affected long-range lattice ordering, revealing a disorder-induced mode at 300 cm^{-1} and a local vibrational mode at 669 cm^{-1} . The low intensities of both modes were shown to scale with Mn concentration. These observations support the formation of nitrogen vacancies, even under optimized MOCVD growth conditions. The slight excess of metal components in the growth process compared to undoped GaN growth and the incorporation of Mn deep acceptor levels favors the formation of nitrogen vacancies relative to undoped GaN. Such vacancies form shallow donor complexes and thus contribute to self-compensation. Electronic defects such as these may be detrimental to the ferromagnetic ordering process. © 2006 American Vacuum Society. [DOI: 10.1116/1.2201052]

The ability to control both flow of charge and spin of charges in electronic devices has been a focus of ferromagnetic research over the past decade. Dilute magnetic semiconductors (DMS) have been studied in pursuit of this goal for use in spintronic devices because of their unique electrical and magnetic properties.¹⁻³ Their similarity to existing semiconductors also shows promise for monolithic integration with existing semiconductor technology. Potential applications include nonvolatile memory, spin-polarized light emitting diodes (spin LEDs), electronic devices with faster switching times and lower power consumption, and elements for solid state quantum computing.^{4,5} However, room temperature operation of spintronic devices has proven elusive.

$\text{Ga}_{1-x}\text{Mn}_x\text{N}$ films that exhibit ferromagnetism at and above room temperature (RT) have recently been realized due to improvements in materials growth technology. RT ferromagnetism has been observed in $\text{Ga}_{1-x}\text{Mn}_x\text{N}$ films grown by metal-oxide chemical vapor deposition (MOCVD),⁶ molecular beam epitaxy (MBE),⁷ and Mn-implanted GaN epilayers.⁸ However, the origin of ferromagnetic behavior is still highly controversial, with several competing theoretical

models that explain the experimental findings.^{1,9-11} Moreover, the possibility of ferromagnetic second phases and/or nanoclusters leads to an increase in the complexity of the study of ferromagnetism in this material system.^{2,12} A ferromagnetic behavior that is closely coupled with the free carriers in the system would be advantageous for most room temperature spintronic devices.^{1,9,10,13}

Hence, a better understanding of the structural properties and the lattice dynamics of Mn-doped GaN epilayers is crucial for understanding the ferromagnetic behavior in this material system and developing a device technology. This article reports the effect of Mn incorporation in $\text{Ga}_{1-x}\text{Mn}_x\text{N}$ epilayers. The long-range and local lattice ordering is investigated for MOCVD-grown $\text{Ga}_{1-x}\text{Mn}_x\text{N}$ and ion-implanted MOCVD-grown GaN. The data show that Mn incorporation into the GaN host lattice reduces long-range lattice ordering and leads to an increase in the formation of nitrogen vacancies. The reduction in long-range lattice ordering can be minimized by MOCVD growth as compared to ion implantation, and the formation of nitrogen vacancies can be reduced with donor-type (e.g., Si) codoping.

$\text{Ga}_{1-x}\text{Mn}_x\text{N}$ layers were produced by MOCVD. Mn ions were also implanted into MOCVD-grown undoped, *p*-

^{a)}Electronic mail: ianf@ece.gatech.edu

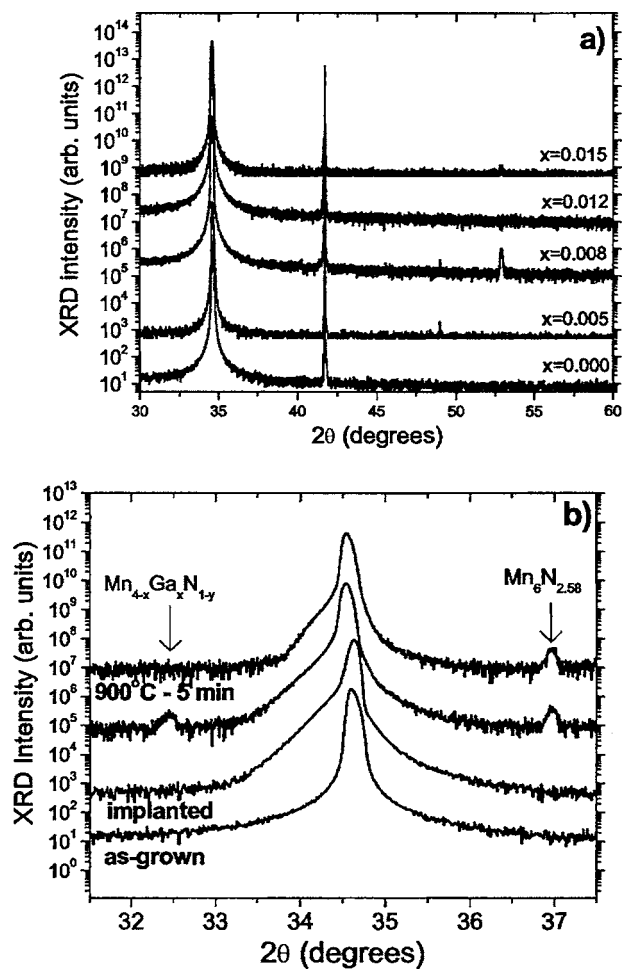


FIG. 1. (a) XRD spectra of the sample series from 0% to 1.5%. Note that no second phases are seen within the resolution of the technique. The small peak at 53° is a $\lambda/2$ remnant of the GaN (0006) reflection. (b) shows a nominally undoped implanted GaN sample before and after annealing. Note the considerable low angle peak asymmetry due to implantation damage and Mn-interstitial introduction.

and *n*-type GaN epilayers with an energy of 200 keV at 400°C . A Mn ion dose of $3 \times 10^{16} \text{ cm}^{-2}$ was used. Base line samples consisted of undoped MOCVD-grown GaN epilayers. The epilayers were grown using a highly modified vertical MOCVD system. $\text{Ga}_{1-x}\text{Mn}_x\text{N}$ layers fabricated via Mn ion implantation were held at 400°C during the implantation process in order to promote dynamic lattice recovery. The implanted samples were subsequently annealed for 4 min at temperatures up to 900°C for complete lattice recovery. A Renishaw micro-Raman system with a 488 nm excitation source was used for Raman measurements. The x-ray diffraction (XRD) analysis was performed using a Philips X'Pert Pro diffractometer.

The results from the x-ray diffraction analysis, electron spin paramagnetic resonance,¹⁴ and the magnetization measurements rule out a high concentration of precipitates in the samples.^{6,15–19} No asymmetrical broadening in the MOCVD-grown GaN peaks was observed in XRD studies.¹⁴ Second phases in the epilayers were below the detection limit as seen in the ω - 2θ scans for the MOCVD-grown samples (Fig. 1), even at the highest Mn concentration of 1.5%. No statistically significant deviation in the *a*- or *c*-axis lattice parameters was observed in the as-grown samples. Figure 1 also shows the pre- and postannealing XRD scans of the implanted samples. The dominant feature in these scans is the pronounced low angle asymmetry in the GaN (0002) peak indicating a remaining lattice damage or a Mn phase.

A more detailed study of the local and long-range lattice properties was performed by Raman spectroscopy. Figure 2 shows Raman spectra for the as-grown $\text{Ga}_{1-x}\text{Mn}_x\text{N}$ samples and the ion-implanted samples. The spectra are dominated by the GaN E_2 (high) mode at 569 cm^{-1} . This peak is shifted by 2 cm^{-1} from the relaxed value of 567 cm^{-1} , most likely due to tensile strain as a result of the growth on sapphire substrates. Comparison of the measured Raman spectra with phonon-dispersion curves for hexagonal GaN shows that the broad peak at 300 cm^{-1} is a disorder-activated mode attributed to the highest acoustic phonon branch.^{20,21} Other Raman

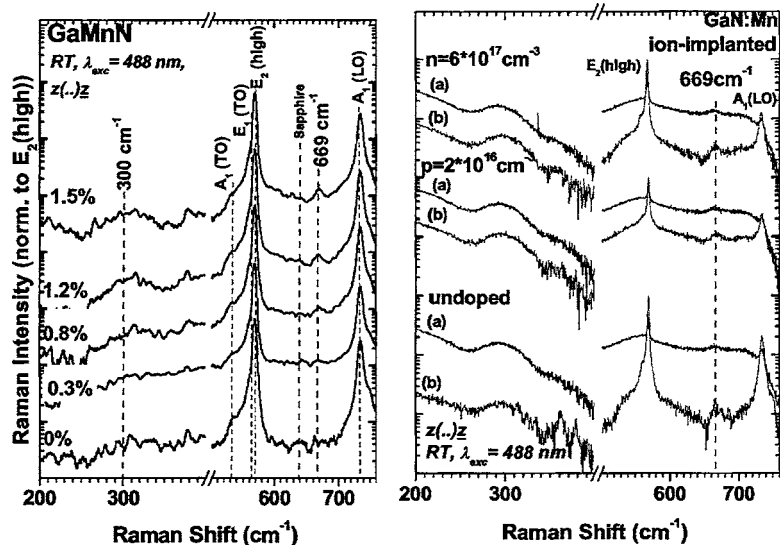


FIG. 2. Raman spectra of MOCVD-grown (left) and ion-implanted GaN:Mn epilayers (right). In both cases, the spectrum is dominated by the GaN E_2 (high) mode. This makes the shift in the $A_1(\text{TO})$ mode that is apparent in FIR spectra much harder to detect in the Raman spectrum. The modes around 160 , 300 , and 670 cm^{-1} are disorder activated. The Mn ions were implanted into *n*-type, *p*-type, and nominally undoped MOCVD-grown GaN epilayers (a). The carrier concentrations are indicated labeling the spectra (shifted vertically for clarity). Raman spectra were also recorded after a 5 min RTA treatment at 700°C in nitrogen atmosphere (b). The same base lines were chosen for the spectra of the as-implanted and the annealed samples, respectively.

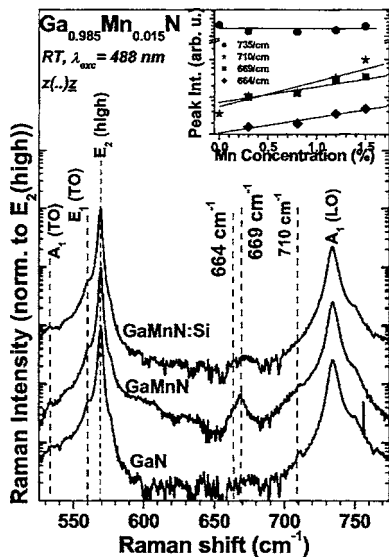


FIG. 3. Sensitivity of the vacancy-induced local vibrational mode (LVM) at 669 cm^{-1} on codoping. Magnesium was used for acceptor codoping, and Silicon was applied to create shallow donors in $\text{Ga}_{0.985}\text{Mn}_{0.015}\text{N}$. Intensity of the vacancy-induced LVMs and the disorder-activated mode near 670 and at 710 cm^{-1} are shown as a function of the Mn concentration in the inset. The intensity of the $A_1(\text{LO})$ mode does not depend on the Mn concentration and is shown for comparison. Note the semilogarithmic plot for the modes at 664 , 669 , and 710 cm^{-1} . The lines are guide to the eye only.

modes detected at 735 , 560 , and 533 cm^{-1} [$A_1(\text{LO})$, $E_1(\text{TO})$, and $A_1(\text{TO})$, respectively] were assigned to the GaN host lattice. The presence of a strong $A_1(\text{LO})$ mode confirms the absence of free carriers within this system due to the large binding energy of the Mn acceptors.²² A slight blueshift (hardening) of the $E_1(\text{TO})$ mode was observed with increasing Mn concentration. However, low Raman scattering intensity prevented further studies. Far infrared (FIR) reflection studies that are more sensitive to the $E_1(\text{TO})$ phonon than Raman backscattering confirmed the observed tendency of lattice hardening with increasing Mn concentration.²³

This study focuses on the Raman modes around 300 and 669 cm^{-1} , which appeared to be more sensitive to Mn incorporation. The intensities of these modes increase with Mn concentration, but no significant shift in their mode energies was observed, and similar behavior was detected for a shoulder near 710 cm^{-1} . The 300 cm^{-1} Mn disorder-activated mode results from defect densities that cause a loss of wave vector conservation in the scattering process.^{20,21} This mode was also observed with significantly higher intensity in the ion-implanted GaN epilayers. Annealing at $700\text{ }^\circ\text{C}$ reduced its intensity, and the Raman spectra became similar to those of the MOCVD-grown $\text{Ga}_{1-x}\text{Mn}_x\text{N}$ epilayers. However, the anneal could not completely remove this lattice disorder. It should be noted that in this work the intensity of these modes is significantly lower [normalized to the E_2 (high) mode] compared to other reports, suggesting that MOCVD growth results in the generation of less lattice disorder due to Mn incorporation.^{20,21,24,25}

The features near 669 cm^{-1} were studied in more detail, as shown in Fig. 3. An asymmetric broadening of this mode

revealed a substructure that can be fitted with an additional mode at 664 cm^{-1} . These modes have previously been attributed to local vibrational modes (LVM) due to vacancies.^{20,21,24,25} This mode is assigned to nitrogen vacancies and depends on the growth conditions. The increase in metal components (e.g., Mn) relative to undoped GaN MOCVD growth conditions preferentially supports the generation of nitrogen vacancies and Mn interstitials in the epilayers. Doping considerations outlined by Zunger²⁶ provided a further argument for this assignment. Most GaN films are intrinsically *n* type because of native defects in the material. With a high concentration of a deep acceptor level dopant, as is the case for Mn concentrations up to 1.5% , the Fermi level shifts toward the Mn deep acceptor level and valence band. The addition of a deep acceptor level (e.g., Mn) during GaN growth causes the formation of donorlike defects such as gallium interstitials and nitrogen vacancies to self-compensate the acceptor-type defects as the Fermi level shifts toward the valence band. First principles calculations have shown that Ga interstitials have a higher formation energy in *p*-type GaN than nitrogen vacancies, making nitrogen vacancies a probable compensation center under acceptor doping conditions.²⁷ This is supported by the Hall characterization of these samples determining them as either residually *n* type or highly resistive. Vacancy formation is also suggested by the infrared reflection data which shows a weakening of the GaN lattice with heavy Mn incorporation,²³ and has been suggested as the predominant self-compensation mechanism in ion-implanted *p*-GaN.²⁸ A high vacancy concentration could also result in the observed decrease in lattice parameter with Mn doping via MBE,²⁹ whereas based on strictly atomic radii considerations an increase in lattice parameter would be expected.

Si codoping produces shallow donor states in GaN that can suppress the formation of nitrogen vacancies by compensating the *p*-type deep level defects introduced by substitutional Mn. Figure 3 shows that Si incorporation during GaN growth suppresses the LVM at 669 cm^{-1} . The importance of the donor presence during the growth process is underscored by a comparison to the ion-implanted samples (see Fig. 2), where no suppression of the vacancy-induced LVM was observed for the *n*-type sample.

The intensities of the modes at 664 , 669 , and 710 cm^{-1} were found to be strongly dependent on Mn concentration (inset of Fig. 3). The $A_1(\text{LO})$ mode is shown for comparison since its intensity does not change with Mn concentration. While the 710 cm^{-1} mode scales even more with Mn concentration, a direct assignment to a Mn-related vibrational mode is not likely since this mode is also observed in, for example, Cu-doped GaN.³⁰ According to theoretical considerations, this mode is due to the mixing of Raman modes from different points of the Brillouin zone.³¹

No feature around 580 cm^{-1} was observed in the Raman spectra that could be assigned to Mn substitution in GaN, unlike the report by Harima.²⁵ However, substitutional Mn incorporation has been confirmed by further studies on these samples,^{6,16,17,19} and several observations are inconsistent

with RT ferromagnetism due to clustering mechanisms. The paramagnetic nature of the Mn sample in Ref. 25 could easily result from substitutional Mn in the d^5 configuration, as is observed in MOCVD-grown material with high Si concentration.¹⁶ Nitrogen vacancies, in particular, like shallow donor complexes such as Si, help to drive the Fermi level above the $Mn^{2+/3+}$ deep acceptor level. The increase in vacancy concentration with Mn doping explains the much larger observed drop in the Bohr-magneton moment per atom μ_B/Mn than would be expected from increased random Mn–Mn antiferromagnetic superexchange interactions.^{6,29} This further demonstrates the need for understanding the electronic as well as structural configuration when reporting the magnetic behavior in these materials.

In conclusion, Raman spectroscopy studies confirmed that the effect of Mn incorporation on the long-range lattice ordering of $Ga_{1-x}Mn_xN$ films ($x < 0.015$) can be minimized by MOCVD growth compared to ion implantation. The formation of nitrogen vacancies as self-compensating centers was evidenced by the behavior of the LVM at 669 cm^{-1} , whose intensity was found to scale with Mn concentration.

ACKNOWLEDGMENTS

One of the authors (M.S.) gratefully acknowledges the support from the Alexander von Humboldt-foundation. Another author (M.H.K.) was supported by the United States Department of Defense through a National Defense Science and Engineering Graduate Fellowship. The authors are grateful to U. Haboeck and A. Hoffmann from the TU Berlin, Germany, for fruitful discussions.

¹T. Dietl, H. Ohno, F. Matsukura, J. Cibert, and D. Ferrand, *Science* **287**, 1019 (2000).

²S. J. Pearton, C. R. Abernathy, M. E. Overberg, G. T. Thaler, and D. P. Norton, *J. Appl. Phys.* **93**, 1 (2003).

³T. Dietl, *Phys. Status Solidi B* **240**, 433 (2003).

⁴S. A. Wolf, D. D. Awschalom, R. A. Buhrman, J. M. Daughton, S. von Molnar, M. L. Roukes, A. Y. Chtchelkanova, and D. Treger, *Science* **294**, 1488 (2001).

⁵D. Loss and D. P. DiVincenzo, *Phys. Rev. A* **57**, 120 (1998).

⁶M. H. Kane *et al.*, *Semicond. Sci. Technol.* **20**, L5 (2005).

⁷M. E. Overberg, C. R. Abernathy, S. J. Pearton, N. A. Theodoropoulou, K. T. McCarthy, and A. F. Hebard, *Appl. Phys. Lett.* **79**, 1312 (2001).

⁸Y. Shon, Y. H. Kwon, D. Y. Kim, D. Fu, and T. W. Kang, *Jpn. J. Appl. Phys., Part 1* **40**, 5304 (2001).

⁹M. Berciu and R. N. Bhatt, *Phys. Rev. Lett.* **87**, 107203 (2001).

¹⁰K. Sato and H. Katayama-Yoshida, *Semicond. Sci. Technol.* **17**, 367 (2002).

¹¹J. M. D. Coey, M. Venkatesan, and C. B. Fitzgerald, *Nat. Mater.* **4**, 173 (2005).

¹²B. K. Rao and P. Jena, *Phys. Rev. Lett.* **89**, 185504 (2002).

¹³A. Lewicki, J. Spalek, J. K. Furdyna, and R. R. Galazka, *Phys. Rev. B* **37**, 1860 (1988).

¹⁴S. Pignard, K. Yu-Zhang, Y. Leprince-Wang, K. Han, H. Vincent, and J. P. Senateur, *Thin Solid Films* **391**, 21 (2001).

¹⁵M. H. Kane *et al.*, in *GaN, AlN, InN and Their Alloys*, MRS Symposia Proceedings No. 831, edited by C. Wetzel, B. Gil, M. Kazuhara, and M. Manfra (Materials Research Society, Warredale, PA, 2005), P.E.9.4.1.

¹⁶M. Strassburg *et al.*, in *GaN, AlN, InN and Their Alloys*, MRS Symposia Proceedings No. 831, edited by C. Wetzel, B. Gil, M. Kazuhara, and M. Manfra (Materials Research Society, Warredale, PA, 2005), P.E.9.5.1.

¹⁷M. Strassburg *et al.*, *J. Phys.: Condens. Matter* **18**, 2615 (2005).

¹⁸M. H. Kane *et al.*, *Phys. Status Solidi C* **2**, 2441 (2005).

¹⁹M. H. Kane, M. Strassburg, W. E. Fenwick, A. Asghar, and I. T. Ferguson, *Int. J. High Speed Electron. Syst.* (submitted).

²⁰W. Limmer, W. Ritter, R. Sauer, B. Mensching, C. Liu, and R. Rauschenbach, *Appl. Phys. Lett.* **72**, 2589 (1998).

²¹M. Zajac *et al.*, *Appl. Phys. Lett.* **78**, 1276 (2001).

²²U. Haboeck, H. Siegle, A. Hoffmann, and C. Thomsen, *Phys. Status Solidi C* **0**, 1710 (2003).

²³Z. G. Hu, M. Strassburg, N. Dietz, A. G. U. Perera, M. H. Kane, A. Asghar, and I. T. Ferguson, *Appl. Phys. Lett.* (to be published).

²⁴W. Gebicki, J. Strzeszewski, G. Kamler, T. Szyszko, and S. Podsiadlo, *Appl. Phys. Lett.* **76**, 3870 (2000).

²⁵H. Harima, *Appl. Phys. Lett.* **16**, S5653 (2004).

²⁶A. Zunger, *Appl. Phys. Lett.* **83**, 57 (2003).

²⁷C. G. Van del Walle and J. Neugebauer, *J. Appl. Phys.* **95**, 3851 (2004).

²⁸Y. Shon *et al.*, *Appl. Phys. Lett.* **81**, 1845 (2002).

²⁹M. L. Reed, E. A. Berkman, M. J. Reed, F. E. Arkun, T. Chikyow, S. M. Bedair, J. M. Zavada, and N. A. El-Masry, in *GaN and Related Alloys*, MRS Symposia Proceedings No. 798, edited by H. M. Ng, M. Wraback, K. Hiramatsu, and N. Grandjean (Materials Research Society, 2004), P.Y.6.1.

³⁰J. Senawirante, M. Strassburg, A. M. Payne, A. Asghar, N. Dietz, and I. T. Ferguson, *Appl. Phys. Lett.* (submitted).

³¹M. M. Bulbul, S. R. P. Smith, B. Obradovic, T. S. Cheng, and C. T. Foxon, *Eur. Phys. J. B* **14**, 423 (2000).